

# Electrocatalysis of oxygen reduction at polypyrrole modified glassy carbon electrode in anthraquinone solutions

Paramasivam Manisankar<sup>a,\*</sup>, Anandhan Gomathi<sup>b</sup>

<sup>a</sup> Department of Chemistry, Periyar University, Salem 636011, Tamil Nadu, India

<sup>b</sup> Department of Industrial Chemistry, Alagappa University, Karaikudi 630003, Tamil Nadu, India

Received 26 November 2004; received in revised form 2 January 2005; accepted 2 January 2005

## Abstract

The electrocatalytic reduction of dioxygen by anthra-9,10-quinone derivatives and dyes at polypyrrole modified glassy carbon electrodes has been investigated. The stability and electrochemical behaviour of the modified electrodes were examined at different pH media and pH 7.0 was chosen as the optimum working pH to study the electrocatalysis by comparing the shift in oxygen reduction potential and enhancement in peak current for oxygen reduction. Anthra-9,10-quinones combined with polypyrrole showed excellent electrocatalytic ability for the reduction of O<sub>2</sub> to H<sub>2</sub>O<sub>2</sub> with overpotentials ranging from 320 to 665 mV in the anodic direction compared to bare glassy carbon electrode. The diffusion coefficient values of anthraquinones at the modified electrodes and the number of electrons involved in anthraquinone reduction were evaluated by chronoamperometric and chronocoulometric techniques, respectively. In addition, chronocoulometric and hydrodynamic voltammetric studies showed the involvement of two electrons in O<sub>2</sub> reduction. The mass specific activity of anthraquinones used, the diffusion coefficient of oxygen and the heterogeneous rate constants for the oxygen reduction at the surface of modified electrodes were also determined by rotating disk voltammetry.

© 2005 Elsevier B.V. All rights reserved.

**Keywords:** Dioxygen reduction; Electrocatalytic reduction; Polypyrrole modified electrodes; Voltammograms; Anthraquinones

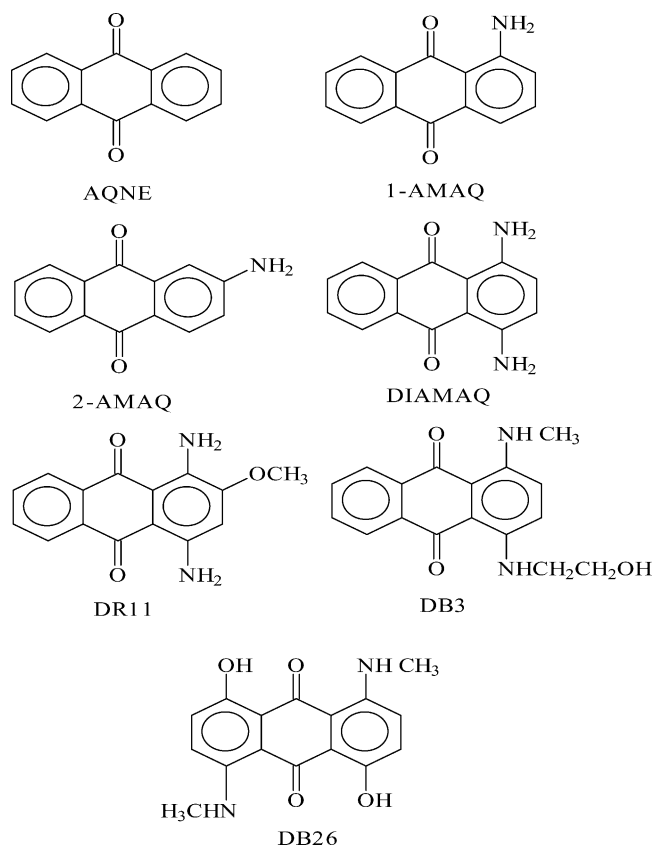
## 1. Introduction

Oxygen reduction finds wide applications in electrochemical technologies such as fuel cell and biosensors [1–5]. The electrocatalytic reduction of oxygen on redox polymer coated electrodes has been the object of active investigation over the past two decades [6–9]. As the catalytic properties depend on propagation of charge through the coating, redox polymer coated electrodes, due to the immobilization of conducting solid polymer at the electrode surface, appear as particularly attractive modified electrodes for the electrocatalytic reductions. Kingsborough and Swager [7] and Ramirez et al. [6] studied the electrocatalytic oxygen reduction at polythiophene-cobalt salen hybrid modified GCE and at poly-

iron-tetra amino phthalocyanine coated GCE, respectively. The catalytic reduction of oxygen was also carried out by Li et al. on Pt particles dispersed on poly (*o*-phenylenediamine) film modified GCE [9].

Many mediators such as copper [10], manganese oxide [11], ruthenium–iron cluster [12], titanium silicates [13], Au nanoparticle [14], metal phthalocyanine [6], metal macrocyclic complexes [1,15], pyrimidine bases [16], naphthoquinone [17,18] and anthraquinone [19–22] derivatives were employed as electrocatalysts for the reduction of dioxygen to water or H<sub>2</sub>O<sub>2</sub>. With redox polymer coatings, high local concentrations of catalytic sites can be achieved, even though the total amount of catalyst remains small. Recently, Singh et al. reported the electrocatalytic activity of composite films of polypyrrole and CoFe<sub>2</sub>O<sub>4</sub> nanoparticles towards O<sub>2</sub> reduction [23]. However, the combined effect of polypyrrole and metal free compounds like anthra-9,10-quinone in

\* Corresponding author. Tel.: +91 427 2345766; fax: +91 427 2345565.  
E-mail address: [pms11@rediffmail.com](mailto:pms11@rediffmail.com) (P. Manisankar).



Scheme 1. Structures of the anthraquinones used.

dioxygen reduction has not been explored so far. Considering the growing importance of quinones as catalysts, many studies have been carried out using mediators with quinonic functions. Salimi et al. reported the electrocatalytic ability of the adsorbed 1,4-dihydroxy anthra-9,10-quinone derivatives [21] and anthraquinone podands [22] on glassy carbon electrodes towards the  $O_2$  reduction with overpotentials from 560 to 650 mV at pH 6.0–7.0 and from 380 to 470 mV at pH 4.5, respectively, lower than that of a bare glassy carbon electrode. In this direction, the glassy carbon electrode has been modified with polypyrrole and used for electrocatalytic reduction of oxygen in the presence of some anthra-9,10-quinones.

In the present investigation, the electrochemical behaviour of anthra-9,10-quinone, its amino derivatives and dyes (Scheme 1) at polypyrrole modified glassy carbon electrode (PPY/GCE), the stability and efficiency of such combination in the electrocatalysis of dioxygen reduction were examined by cyclic voltammetry, chronoamperometry, chronocoulometry and rotating disk voltammetry along with the determination of diffusional and kinetic parameters.

## 2. Experimental

Anthra-9,10-quinone (AQNE), 1-amino anthra-9,10-quinone (1-AMAQ), 2-amino anthra-9,10-quinone (2-AMAQ)

and 1,4-diamino anthra-9,10-quinone (DIAMAQ) were purchased from Lancaster. 1-[(2-Hydroxy ethyl)amino]-4-(methyl amino) anthra-9,10-quinone (DB3), 1,5-dihydroxy-4,8-bis(methyl amino) anthra-9,10-quinone (DB26) and 1,4-diamino-2-methoxy anthra-9,10-quinone (DR11) were received as samples from ATUL India Ltd. and purified before use. The experimental solutions of anthraquinones in acetonitrile of concentration  $1.0 \times 10^{-6} \text{ mol cm}^{-3}$  were prepared. HPLC grade acetonitrile (SRL) was used as received. The 50% aqueous acetonitrile solutions used at different pH values were 0.1 M  $H_2SO_4$  (pH 1.0), 0.1 M  $H_2SO_4$  + 0.1 M NaOH (for pH 2.0–3.0), 0.2 M  $CH_3COOH$  + 0.2 M  $CH_3COONa$  (for pH 4.0–5.0), 0.1 M  $NaH_2PO_4$  + 0.1 M NaOH (for pH 6.0–12.0) and 0.1 M NaOH (pH 13.0). The required values of pH were obtained with the described solutions by mixing and the pH of the media was measured using a Cyberscan 500-pH meter. Triply distilled water deionized by TKA water purifier was used throughout the experiments. All other chemicals used were of the highest purity available from Merck. Nitrogen and oxygen gases with 99.99% purity were used during the experiments.

PPY/GCE was prepared by potentiostatic method in which the glassy carbon electrode was kept in 0.1 M pyrrole solution in acetonitrile containing  $1.5 \times 10^{-2} \text{ g}$  of KCl at 0.9 V (versus Calomel electrode) [24]. Thickness of the film (0.1  $\mu\text{m}$ ) was controlled coulometrically. The coating was removed by polishing followed by cleaning with dilute nitric acid solution.

A three-electrode system containing a saturated calomel reference electrode (SCE), a platinum wire counter electrode and a polypyrrole modified glassy carbon working electrode ( $A = 0.0314 \text{ cm}^2$ ) was kept in the cell solution, which contains anthraquinone derivatives. All electrochemical experiments were performed at a thermostatic temperature of  $25.0 \pm 0.1 \text{ }^\circ\text{C}$ .

An EG&G Princeton Applied Research Model 273A potentiostat/galvanostat (Princeton, NJ, USA) controlled by M270 software was employed to perform cyclic voltammetry, chronoamperometry and chronocoulometry techniques. In all cyclic voltammetric studies, background current was measured at various scan rates and subtracted properly. A Bi-potentiostat model AFRDE5 having an analytical rotator model AFMSRXE with MSRX speed control (PINE Instruments, USA) was used for hydrodynamic voltammetric studies on dioxygen reduction.

## 3. Results and discussion

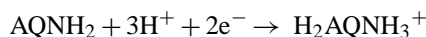
All voltammetric studies of anthra-9,10-quinone, its amino derivatives and dyes were performed at PPY/GCE in the absence and presence of oxygen at various pH media in the range 1.0–13.0.

### 3.1. Electrochemical behaviour of anthra-9,10-quinones at PPY/GCE

Different anthra-9,10-quinones exhibited different cyclic voltammograms under deaerated conditions depending upon the substituents present and nature of anthraquinones. As an example, at pH 7.0, 1-AMAQ and AQNE showed a single redox couple whereas a sharp irreversible cathodic peak was observed for DIAMAQ. 2-AMAQ and DR11 showed very broad irreversible cathodic peak and broad redox couples were obtained for DB3 and DB26. The variation of cathodic peak current with scan rate was studied by performing these voltammograms at various scan rates. Fig. 1 shows the cyclic voltammogram for 1-AMAQ at pH 7.0 and the inset exhibits the linear variation of cathodic peak current ( $I_{pc}$ ) with square root of scan rate ( $v^{1/2}$ ). Moreover, the plot of  $\log I_{pc}$  versus  $\log v$  is a straight line with a slope around 0.5 suggesting the mass transfer as diffusion controlled adsorption [25,26].

#### 3.1.1. Effect of pH

The reduction peak potentials shift cathodically toward more negative values with increase in pH of the solution. Anthraquinones are known to give the corresponding hydroquinone derivatives by reduction in aqueous solutions [21,22]. AQNE undergoes two-electron two-proton reduction to give the hydroquinone up to pH 8.0 and two-electron one-proton reduction process above pH 8.0 to yield hydroquinone anion. At the electrode surface, the remaining six amino anthraquinone derivatives and dyes undergo two-electron three-proton reduction at low pH values to give the corresponding protonated hydroquinones



In DIAMAQ, DB3, DB26 and DR11, the protonation of the second amino group may be difficult due to the presence of electron withdrawing quaternary ammonium cation in protonated anthraquinones. At the intermediate pH range, the anthraquinone derivatives undergo two-electron two-proton

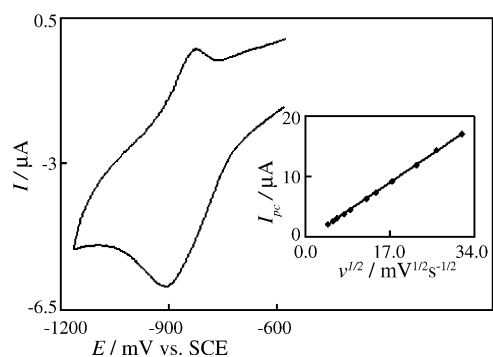
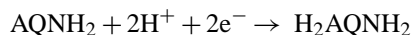
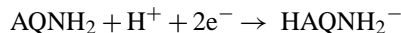


Fig. 1. Cyclic voltammogram of 1-AMAQ at PPY/GCE in phosphate buffer pH 7.0 at scan rate  $40 \text{ mV s}^{-1}$ . The inset shows the plot of the cathodic peak current vs. square root of scan rate.

process producing the corresponding hydroquinones



At  $\text{pH} > 8.0$ , the electrode surface reaction is two-electron one-proton process, which leads to the formation of hydroquinone anion



#### 3.1.2. Stability of the modified electrodes

In order to examine the stability of the modified electrode in the presence of catalyst and the reproducibility of its electrochemical behaviour, the modified electrodes were immersed in acidic medium (pH 1.0) containing the catalyst for 20 h and in neutral medium (pH 7.0) containing anthraquinones for 30 h and then cyclic voltammograms were recorded. In both media, there was a slight decrease in the corresponding voltammograms (<4%). In addition, there were no changes in the peak current or separation of the peak in cyclic voltammograms after 100 cycles of repetitive scanning at scan rate  $40 \text{ mV s}^{-1}$  in pH 7.0 buffer.

### 3.2. Catalytic reduction of dioxygen at the surface of modified electrodes

#### 3.2.1. Effect of pH

The catalytic effect of anthra-9,10-quinones in dioxygen reduction at PPY/GCE was studied in various buffers between pH 1.0 and 13.0. Even though the reduction potentials of dioxygen and anthraquinones are pH-dependent [22], their displacement may be unequal due to their different kinetic behaviour. As the pH of buffer solution increases, there is a gradual increase in the cathodic peak current up to pH 7.0. The optimum pH was found to be 7.0 to study the electrocatalytic reduction of dioxygen because of the maximum cathodic current enhancement and oxygen reduction potential shift observed at this neutral pH. This shift is the difference between the oxygen reduction potential at PPY/GCE with anthraquinone and that at bare GCE without anthraquinone. Shamsipur and co-workers also studied this reduction using GCE modified by 1,4-dihydroxy-anthra-9,10-quinone derivatives only at pH 6.0–7.0 [21]. It is reported recently [3] that dioxygen is reduced bioelectrocatalytically to water at neutral pH.

#### 3.2.2. Stability of the modified electrodes against $\text{O}_2$ reduction

The stability of the modified electrode towards  $\text{O}_2$  reduction was also examined by performing cyclic voltammograms of 100 repetitive cycles at scan rate  $40 \text{ mV s}^{-1}$  in oxygen saturated solution with anthraquinone at pH 7.0. There were no changes in peak potential and current in the successive cycles. After such 100 repetitive cycles, the cyclic voltammogram was carried out in the absence of oxygen and compared with the cyclic voltammogram obtained initially under deaerated

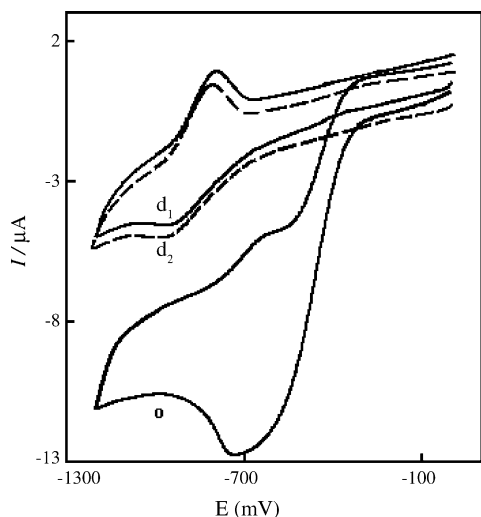
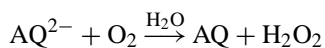
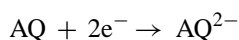


Fig. 2. Cyclic voltammograms of AQNE on PPY/GCE at pH 7.0 under deaerated at the beginning ( $d_1$ , solid line), oxygen saturated (o) and again deaerated ( $d_2$ , dashed line) conditions. Scan rate  $40 \text{ mV s}^{-1}$ .

condition. A 5% decrease in the cathodic peak current without any change in the peak separation was observed. As an illustration, the cyclic voltammograms obtained under deaerated, oxygen saturated and again deaerated conditions are presented in Fig. 2 for the compound AQNE. Thus the stability of the modified electrode against electrocatalytic studies was established.

### 3.2.3. Dioxygen reduction at pH 7.0

Since the reduction of anthraquinones is a diffusion controlled adsorption process, the catalyst molecules approach the surface of the electrode by diffusion and get entrapped in the cavities of polypyrrole film. The adsorbed anthraquinone derivatives and dyes shift the oxygen reduction potential more to anodic side. Being cationic polymer, polypyrrole facilitates the stability of the hydroquinone dianion formed by the reduction of anthraquinones. The combined effect of polypyrrole and anthraquinones towards dioxygen reduction was studied by comparing the voltammograms of oxygen reduction at PPY/GCE with anthraquinones and at bare GCE without anthraquinones. For instance, Fig. 3 shows the cyclic voltammograms of DIAMAQ in the absence and presence of oxygen at pH 7.0. Here, DIAMAQ combined with PPY reduces the oxygen at  $-355.9 \text{ mV}$ . Since dioxygen reduces at  $-1020.9 \text{ mV}$  on bare GCE at pH 7.0, the shift in oxygen reduction potential is found to be  $665 \text{ mV}$ . The probable mechanism for the electrocatalytic reduction of oxygen by adsorbed anthraquinones is given as



As an exemption, 1-AMAQ (Fig. 4) reduces the oxygen at two potentials, viz.  $-592.0$  and  $-952.0 \text{ mV}$  at pH 7.0. The reduction peak at more cathodic side may be due to the reduc-

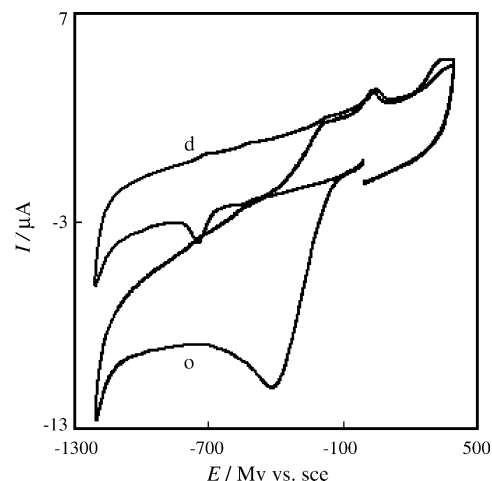
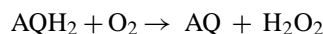
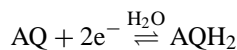


Fig. 3. Cyclic voltammograms of DIAMAQ on PPY/GCE at pH 7.0 in the absence (d) and presence of oxygen (o). Scan rate  $40 \text{ mV s}^{-1}$ .

tion of oxygen by diffused catalytic molecules in which the neutral species hydroanthraquinone catalyzes the  $\text{O}_2$  reduction. The corresponding anodic peak is indicative of partial involvement of hydroquinones in oxygen reduction and the remaining molecules revert to anthraquinone itself. Hence, the possible mechanism for the electrocatalysis of dioxygen by diffused catalytic molecules is summarized as



The observed oxygen reduction potential shifts with the different anthraquinones investigated are about  $320$ – $665 \text{ mV}$  and given in Table 1.

The effect of anthraquinones alone on dioxygen reduction was also studied by comparing the voltammograms of  $\text{O}_2$  reduction in the absence and presence of anthraquinone

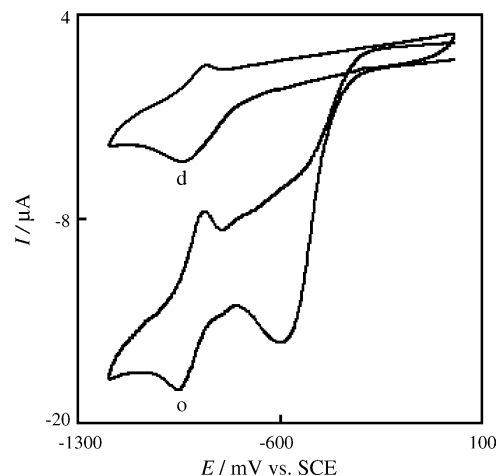


Fig. 4. Cyclic voltammograms of 1-AMAQ on PPY/GCE at pH 7.0 in the absence (d) and presence of oxygen (o). Scan rate  $40 \text{ mV s}^{-1}$ .

Table 1

Diffusion coefficient of anthraquinones  $D_{\text{Aq}}$  (CA), number of electrons involved in the reduction of anthraquinones  $n_{\text{Aq}}$  (CC), potential shift in  $\text{O}_2$  reduction  $\Delta E$  (CV) and number of electrons involved in  $\text{O}_2$  reduction  $n_{\text{O}_2}$  (CC)

Anthraquinones	$D_{\text{Aq}}^{\text{a}}$ ( $\times 10^5 \text{ cm}^2 \text{ s}^{-1}$ )	$n_{\text{Aq}}$	Potential shift $\Delta E$ (mV)		$n_{\text{O}_2}$
			PPY + AQ	AQ	
AQNE	$1.80 \pm 0.06$	2.01	341	62	2.28
1-AMAQ	$1.67 \pm 0.04$	2.01	429	150	2.07
2-AMAQ	$1.62 \pm 0.05$	2.03	321	42	2.01
DIAMAQ	$1.54 \pm 0.04$	2.04	665	386	2.10
DR11	$1.41 \pm 0.02$	2.08	414	135	2.07
DB3	$1.03 \pm 0.04$	2.09	463	184	2.16
DB26	$0.92 \pm 0.03$	2.13	451	172	2.23

<sup>a</sup> The parameters were calculated from four replicate measurements.

derivatives at PPY/GCE and the shifts in  $\text{O}_2$  reduction potential are reported in Table 1. As an example, DIAMAQ on PPY/GCE causes an oxygen reduction potential shift of about 386 mV at pH 7.0.

### 3.2.4. Effect of the substituents towards oxygen reduction

The influence of 9,10-anthraquinone substituents in electrocatalytic properties was investigated by comparing the shift in oxygen reduction potential. The decreasing order of potential shift is DIAMAQ > DB3 > DB26 > 1-AMAQ > DR11 > AQNE > 2-AMAQ. The effect of the substituents has been discussed with regard to the stability of the hydroquinone dianion intermediate. The largest shift observed in DIAMAQ is due to the stabilization of hydroquinone dianion intermediate through the intramolecular H-bonding. But in DB3, inductively electron donating (+I) alkyl groups increase the electron density at nitrogen and cause slight decrease in the hydrogen bond strength. Even though more number of hydrogen bonds is present in DB26, because of peri effect on both sides of oxygen in hydroquinone dianion, the stability of its intermediate is reduced. Due to the presence of only one intramolecular H-bonding between  $-\text{NH}_2$  and one of the hydroquinone oxygen, 1-AMAQ showed lesser shift as compared with DIAMAQ, DB3 and DB26. In DR11, steric effect exerted by the *o*-substituent  $-\text{OCH}_3$  causes the still lower potential shift. The absence of intramolecular hydrogen bonding decreases the stability of intermediates in AQNE and 2-AMAQ. In addition, the unsymmetrical structure of 2-AMAQ causes the oxygen reduction potential shift to the least extent.

### 3.3. Chronoamperometric studies

The chronoamperometric behaviour of PPY/GCE with anthra-9,10-quinones was studied in the absence and presence of oxygen using the double potential-step technique with an initial and final potential of  $-100$  and  $-800$  mV versus SCE, respectively. As an example, the chronoamperograms of bare GCE and GCE modified by polypyrrole with DB26 in

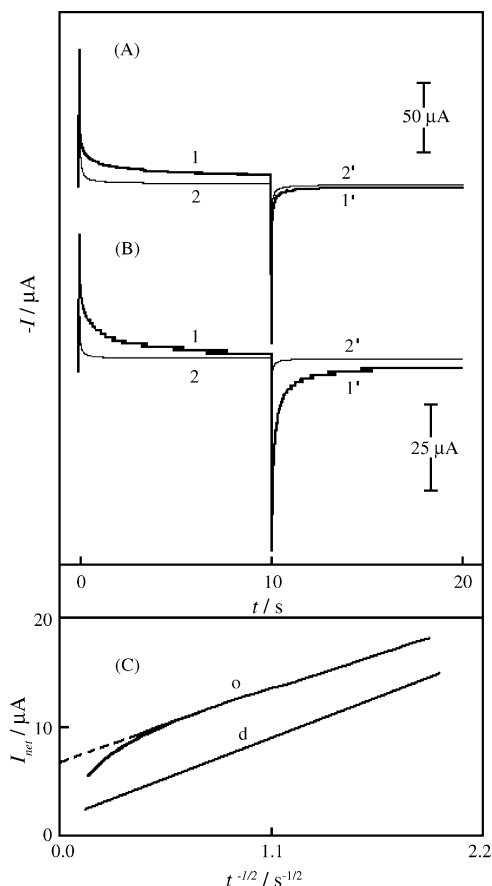


Fig. 5. Chronoamperograms obtained in pH 7.0 by the double potential-step technique at an initial potential of  $-100$  mV and final potential of  $-800$  mV vs. SCE. (A) 1, 1' for modified GCE by PPY and DB26 in the  $\text{O}_2$ -saturated buffer. 2, 2' as 1, 1' for the bare GCE. (B) 1, 1' for modified GCE by PPY and DB26 under deaerated condition, 2, 2' as 1, 1' for the bare GCE. (C) Plots of net current vs.  $t^{-1/2}$  for the above-modified GCE in the absence (d) and presence (o) of dioxygen.

the presence and absence of oxygen are represented in Fig. 5A and B, respectively. The net current  $I_{\text{net}}$  was obtained by point-to-point subtraction of the background current from the current observed for the modified electrodes in the presence and absence of oxygen. In deoxygenated buffer, the plot of net current versus  $t^{-1/2}$  shows a straight line (Fig. 5C, line d) which extrapolates close to the origin. From the slope of Cottrell plot, the diffusion coefficient values of anthraquinones used were determined using the Cottrell equation

$$I = nFD^{1/2}AC_{\text{Aq}}\pi^{-1/2}t^{-1/2},$$

$$\text{slope} = nFD^{1/2}AC_{\text{Aq}}\pi^{-1/2}$$

where  $C_{\text{Aq}}$  is the concentration of the anthraquinone used ( $1.82 \times 10^{-7} \text{ mol cm}^{-3}$ ),  $D$  is the diffusion coefficient of anthraquinone and  $A$  is the geometric area ( $0.0314 \text{ cm}^2$ ) of the glassy carbon electrode. The calculated  $D$  values are summarized in Table 1.

In oxygenated buffer, the corresponding Cottrell plot  $I_{\text{net}}$  versus  $t^{-1/2}$  (Fig. 5C, line o) is linear at short time periods while it deviates from the linearity at longer times. The ex-

trapolation of linear part of the plot results an intercept at  $6.71 \mu\text{A}$ . This transient current largely seems to be due to the catalytic reduction of  $\text{O}_2$  by DB26 and PPY, since the direct reduction of oxygen at blank electrode under the same experimental conditions shows only a little residual current. Similar behaviour was observed in the case of other anthraquinones used.

### 3.4. Chronocoulometric studies

Double potential-step chronocoulometric studies were performed with anthra-9,10-quinones using PPY/GCE in the absence and presence of oxygen with an initial and final potential of  $-100$  and  $-800$  mV versus SCE, respectively. An example of chronocoulomogram for DB3 at PPY/GCE in the presence and absence of  $\text{O}_2$  at pH 7.0 is illustrated in Fig. 6. Under oxygen saturated conditions, large enhancement of charge and the appearance of nearly flat line compared to deaerated condition when the potential is reversed, prove an irreversible electrocatalytic reduction of oxygen. The same behaviour was observed for the other anthraquinones used.

The number of electrons ( $n$ ) involved in the reduction of anthraquinones at the optimum pH was calculated from the slope of  $Q$  versus  $t^{1/2}$  plots under deaerated conditions, using the Cottrell equation,

$$Q = 2nFACD^{1/2}\pi^{-1/2}t^{1/2}$$

by employing the diffusion coefficient values of anthraquinones obtained from chronoamperometric results. The calculated  $n$  values are closer to 2.0 and presented in Table 1. The number of the electrons ( $n$ ) involved in dioxygen reduction at PPY/GCE with anthraquinones was also determined as 2.0 (Table 1) from the slope of  $Q$  versus  $t^{1/2}$  plots under oxygen saturated conditions when  $C = 1.25$  mM,  $A = 0.0314$  cm<sup>2</sup> and  $D = 1.57 \times 10^{-5}$  cm<sup>2</sup> s<sup>-1</sup>. Hence the reduction product is hydrogen peroxide [17,21,22].

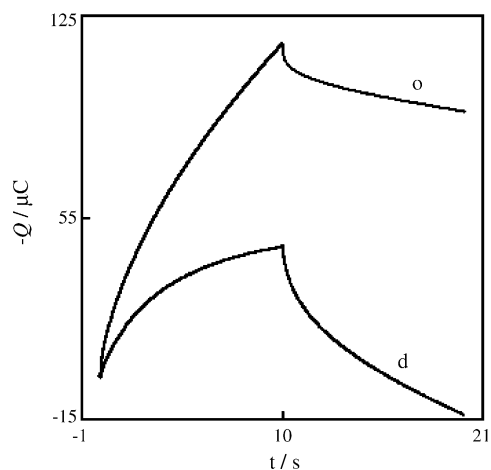


Fig. 6. Chronocoulometric curves of DB3 at PPY/GCE (pH 7.0) in the absence (d) and presence of (o) oxygen.

### 3.5. Hydrodynamic voltammetric studies

The electrocatalytic reduction of  $\text{O}_2$  was also carried out at rotating polypyrrole modified GC electrodes with anthraquinones at the optimum pH 7.0 to assess the kinetic parameters more quantitatively. As an example, a set of current–potential curves recorded in an  $\text{O}_2$  saturated buffer of pH 7.0 at various angular velocities  $\omega$ , with a rotating disk glassy carbon electrode modified by polypyrrole in the presence of DIAMAQ are shown in Fig. 7A. The Levich and Koutecky–Levich plots were made from the limiting current measured at a potential  $-950$  mV and are shown in Fig. 7B and C respectively. The Levich plot in Fig. 7B is very close to the theoretically calculated line for a two electron process ( $n=2$ ) and shows slight negative deviation at higher  $\omega$  values. This non-linearity may be the result of a catalyzed reduction in which a current limiting chemical step precedes the electron transfer [17,22]. The

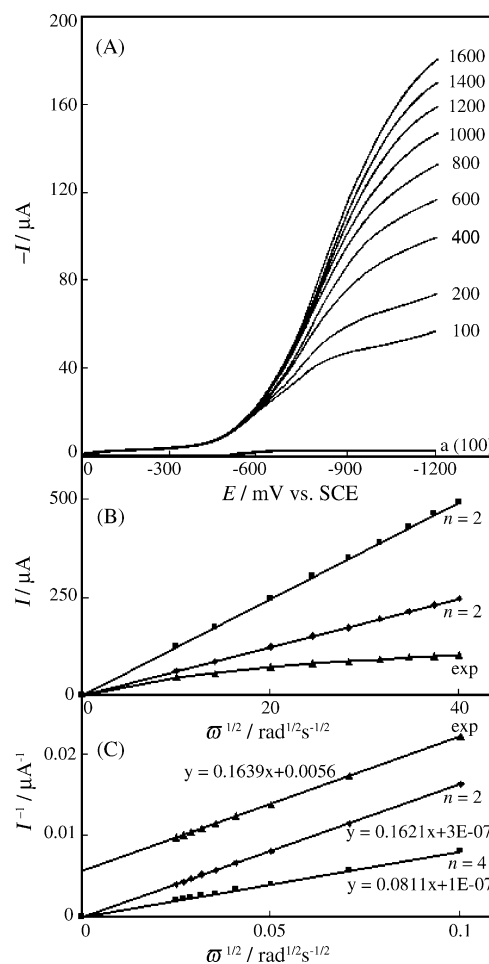


Fig. 7. (A) Current–potential curves for the reduction of  $\text{O}_2$  (1.25 mM) in the presence of DIAMAQ at a rotating glassy carbon electrode modified with polypyrrole in the buffered solution of pH 7.0 at different rotation rates (rpm) and scan rate  $20 \text{ mV s}^{-1}$ , (B) Levich plots of limiting currents at  $-950$  mV (exp), and theoretical Levich plots for two ( $n=2$ ) and four ( $n=4$ ) electron reduction of  $\text{O}_2$ , (C) Koutecky–Levich plots of the above data.

Table 2

Surface coverage  $\Gamma_{\text{Aq}}$ , mass specific current (MSC), heterogeneous rate constant  $k$ , and diffusion coefficient of  $\text{O}_2$  ( $D_{\text{O}_2}$ ) in the electrocatalytic reduction of  $\text{O}_2$  at the surface of polypyrrole modified electrodes

Anthraquinones	$\Gamma_{\text{Aq}}$ ( $\times 10^9 \text{ mol cm}^{-2}$ )	MSC ( $\text{A mg}^{-1}$ )	$k^a$ ( $\times 10^{-4} \text{ M}^{-1} \text{ s}^{-1}$ )	$D_{\text{O}_2}^a$ ( $\times 10^5 \text{ cm}^2 \text{ s}^{-1}$ )
AQNE	1.31	6.09	$3.48 \pm 0.05$	$1.49 \pm 0.03$
1-AMAQ	2.09	3.83	$4.21 \pm 0.08$	$1.49 \pm 0.05$
2-AMAQ	–	–	–	–
DIAMAQ	0.45	13.41	$5.20 \pm 0.07$	$1.48 \pm 0.02$
DR11	–	–	–	–
DB3	2.08	2.90	$4.87 \pm 0.12$	$1.46 \pm 0.04$
DB26	2.07	2.89	$4.55 \pm 0.14$	$1.47 \pm 0.03$

<sup>a</sup> The parameters were calculated from four replicate measurements.

corresponding Koutecky–Levich plot in Fig. 7C is linear, with a slope close to that of the theoretical line for two electron  $\text{O}_2$  reduction. This supports the accomplishment of the catalytic reduction of  $\text{O}_2$  to  $\text{H}_2\text{O}_2$  at PPY/GCE by DIAMAQ. Similar behaviour was observed for the case of other 9,10-anthraquinones used. The mass specific activity of anthraquinones, which is defined as current response of the catalyst per mg in dioxygen reduction, at  $\omega = 100 \text{ rpm}$  was determined [27] and is represented in Table 2. The heterogeneous rate constant for the catalytic reaction between the reduced anthraquinone and oxygen is evaluated from the intercepts of Koutecky–Levich plot using the expression [17,18,21,22]

$$I_1^{-1} = I_k^{-1} + I_{\text{lev}}^{-1} = [nFAkC_{\text{O}_2}\Gamma_{\text{Aq}}]^{-1} + [0.62nFAD_{\text{O}_2}^{2/3}\nu^{-1/6}\omega^{1/2}C_{\text{O}_2}]^{-1}$$

where  $C_{\text{O}_2}$  is the bulk concentration of  $\text{O}_2$  (1.25 mM),  $\omega$  is the rotational speed,  $\nu$  is the hydrodynamic viscosity ( $0.01 \text{ cm}^2 \text{ s}^{-1}$ ),  $\Gamma_{\text{Aq}}$  is the electrode surface coverage of the corresponding anthraquinone,  $k$  is the rate constant and all the remaining parameters have their usual meanings. The surface coverage  $\Gamma_{\text{Aq}}$  can be evaluated from the equation  $\Gamma_{\text{Aq}} = Q/nFA$ , where  $Q$  is the charge obtained by integrating the cathodic peak under the background correction at low scan rate of  $10 \text{ mV s}^{-1}$  and the other symbols have their usual meanings. Since the charge  $Q$  could not be predicted for very broad peaks exhibited by 2-AMAQ and DR11, their surface coverage values were not evaluated. The calculated surface coverage  $\Gamma_{\text{Aq}}$  and rate constant values are included in Table 2.

#### 4. Conclusion

9,10-Anthraquinones were employed as electrocatalysts for the reduction of dioxygen to hydrogen peroxide at polypyrrole modified GCE. Anthraquinones combined with polypyrrole exhibited potent electrocatalytic activities towards oxygen reduction in the neutral pH 7.0 with over potential of about 320–665 mV in the anodic direction compared to bare GC electrode. These shifts are larger than the values reported for GC electrodes modified with anthraquinone

podands [22] and 1,4-dihydroxy anthraquinones [21]. The adsorbed catalytic molecules reduced the oxygen at lower potential than the diffused molecules. The heterogeneous rate constants of dioxygen reduction determined at these modified electrodes are greater than the previously reported values [21,22]. The diffusion coefficient values of oxygen are also comparable with the earlier reports [17,21,22]. The specificity of these polypyrrole modified electrodes with anthraquinones towards dissolved oxygen suggests their possible use as oxygen sensors.

#### References

- [1] E.L. Dewi, K. Oyaizu, H. Nishide, E. Tsuchida, J. Power Sour. 130 (2004) 286.
- [2] A. Ayad, Y. Naimi, J. Bouet, J.F. Fauvarque, J. Power Sour. 130 (2004) 50.
- [3] S. Tsujimura, M. Kawaharada, T. Nakagawa, K. Kano, T. Ikeda, Electrochem. Commun. 5 (2003) 138.
- [4] M.C. Williams, Fuel Cell Handbook, 5th ed., Department of Energy, Washington, USA, 2000, p. 1.
- [5] H. Naohara, S. Ye, K. Uosaki, Electrochim. Acta 45 (2000) 3305.
- [6] G. Ramirez, E. Trollund, M. Isaacs, F. Armijo, J. Zagal, J. Costamagana, M.J. Aguirre, Electroanalysis 14 (2002) 540.
- [7] R.P. Kingsborough, T.M. Swager, Chem. Mater. 12 (2000) 872.
- [8] V. Ganesan, R. Ramaraj, J. Appl. Electrochem. 30 (2000) 757.
- [9] Y. Li, R. Lenigk, X. Wu, B. Gruendig, S. Dong, R. Renneberg, Electroanalysis 10 (1998) 671.
- [10] M.B. Vukmirovic, N. Vasiljevic, N. Dimitrov, K. Sieradzki, J. Electrochem. Soc. 150 (2003) 10.
- [11] L. Mao, D. Zhang, T. Sotomura, K. Nakatsu, N. Koshiba, T. Ohsaka, Electrochim. Acta 48 (2003) 1015.
- [12] R. Gonzalez-Cruz, O. Solorza-Feria, J. Solid State Electrochem. 7 (2003) 289.
- [13] R. Chithra, R. Renuka, J. Appl. Electrochem. 33 (2003) 443.
- [14] Y. Zhang, S. Asahina, S. Yoshihara, T. Shirakashi, Electrochim. Acta 48 (2003) 741.
- [15] A.S. Lin, J.C. Huang, J. Electroanal. Chem. 541 (2003) 147.
- [16] S. Peressini, C. Tavagnacco, G. Costa, C. Amatore, J. Electroanal. Chem. 532 (2002) 295.
- [17] P. Manisankar, A. Mercy Pushpalatha, S. Vasanthkumar, A. Gomathi, S. Viswanathan, J. Electroanal. Chem. 571 (2004) 43.
- [18] S. Golabi, J.B. Raoof, J. Electroanal. Chem. 416 (1996) 75.
- [19] A. Sarapu, K. Vaik, D.J. Schiffrin, K. Tammeveski, J. Electroanal. Chem. 541 (2003) 23.
- [20] K. Tammeveski, K. Kontturi, R.J. Nichols, R.J. Potter, D.J. Schiffrin, J. Electroanal. Chem. 515 (2001) 101.
- [21] A. Salimi, M.F. Mousavi, H. Sharghi, M. Shamsipur, Bull. Chem. Soc. Jpn. 72 (1999) 2121.

- [22] A. Salimi, H. Eshghi, H. Sharghi, S.M. Golabi, M. Shamsipur, *Electroanalysis* 11 (1999) 114.
- [23] R.N. Singh, B. Lal, M. Malviya, *Electrochim. Acta* 49 (2004) 4605.
- [24] M. Arca, A. Yildiz, *Electroanalysis* 6 (1994) 79.
- [25] J.A. Osteryoung, J. O'Dea, in: A.J. Bard (Ed.), *Electroanalytical Chemistry*, vol. 14, Marcel Dekker, New York, 1986, p. 209.
- [26] H.G. Prabu, P. Manisankar, *Analyst* 119 (1994) 1867.
- [27] S.R. Brankovic, J.X. Wang, R.R. Adzic, *Electrochem. Solid State Lett.* 4 (2001) 217.